High-speed Ultrahigh Resolution Optical Coherence Tomography before and after Ranibizumab for Age-related Macular Degeneration

Andre J. Witkin, MD[1], **Laurel N. Vuong, BS**[1], **Vivek J. Srinivasan, PhD**[2], **Iwona Gorczynska, PhD**[1,2], **Elias Reichel, MD**[1], **Caroline R. Baumal, MD**[1], **Adam H. Rogers, MD**[1], **Joel S. Schuman, MD**[3], **James G. Fujimoto, PhD**[2], and **Jay S. Duker, MD**[1]

[1] Tufts Medical Center, Boston, Massachusetts.

[2] Massachusetts Institute of Technology, Boston, Massachusetts.

[3] University of Pittsburgh Medical Center, Pittsburgh, Pennsylvania.

Abstract

Objective—To evaluate intraretinal anatomy in patients with exudative age-related macular degeneration (AMD) using high-speed ultrahigh resolution optical coherence tomography (hsUHR-OCT) before and 1 month after intravitreal injection of ranibizumab.

Design—Retrospective case series.

Participants—Twelve eyes of 12 patients.

Methods—A broad bandwidth superluminescent diode laser light source and spectral/Fourier domain signal detection were used to create a prototype hsUHR-OCT instrument with 3.5 μm axial image resolution and approximately 25,000 lines/second acquisition speed. Twelve eyes of 12 patients with exudative AMD were imaged with hsUHR-OCT before and 1 month after intravitreal ranibizumab injection. High pixel density and raster-scanned 3-dimensional (3D) OCT data sets were generated. Three-dimensional imaging software was used to calculate subretinal/retinal pigment epithelium fluid volume and volume of the fibrovascular lesion.

Main Outcome Measures—Qualitative and quantitative analysis of hsUHR-OCT images and 3D data sets.

Results—All eyes had some degree of normalization of macular contour after intravitreal ranibizumab. The inner/outer photoreceptor segment junction visualized on hsUHR-OCT was discontinuous, overlying the fibrovascular lesion in all 12 of 12 eyes both before and after treatment; 9 of 12 eyes had focal areas of thinning of the outer nuclear layer, which remained after treatment. Volumetric measurements were possible in 8 of 12 eyes with 3D-rendering software. Fibrovascular lesion volume did not change significantly after treatment.

Correspondence: Andre J. Witkin, MD, Tufts Medical Center, 800 Washington St, Box 450, Boston, MA 02111. E-mail: AJWitkin@Gmail.com..

Conclusions—hsUHR-OCT is capable of unprecedented imaging speed and resolution, making it a valuable instrument in measuring in vivo intraretinal pathology. All 12 eyes had some normalization of macular contour. Fibrovascular lesion volume did not change significantly 1 month after treatment, suggesting that ranibizumab does not cause much initial regression of preexisting neovascular tissue. Photoreceptor abnormalities remained in all patients after treatment of wet AMD, suggesting that although ranibizumab improves overall retinal architecture, some photoreceptor damage may be irreversible.

Financial Disclosure(s)—Proprietary or commercial disclosure may be found after the references.

Age-related macular degeneration (AMD) is a chronic and degenerative disease and one of the most common causes of legal blindness in developed countries. The neovascular (exudative or wet) form is often devastating to a patient's central vision. Abnormal neovascularization leads to leakage of blood and fluid into and underneath the retina, ultimately causing loss of central vision when involving the macula.[1,2]

Investigators have theorized that a vascular growth factor may be secreted in unusually large amounts to promote aberrant vessel growth in these patients. With the discovery of vascular endothelial growth factor (VEGF) and its subsequent implication in various retinal diseases, including wet AMD, new therapies have been developed that specifically target this molecule. Inhibition of VEGF-A has been shown to be an effective therapy in the treatment of exudative AMD. Ranibizumab, a humanized antibody fragment that targets all forms of VEGF-A, was approved by the Food and Drug Administration in 2006 for treatment of all types of exudative AMD in the United States.[1,2]

Two large phase 3 studies, the Minimally Classic/Occult Trial of the Anti-VEGF Antibody Ranibizumab in the Treatment of Neovascular AMD (MARINA) and Anti-VEGF Antibody for the Treatment of Predominantly Classic Choroidal Neovascularization in AMD (ANCHOR) trials, showed stabilization or improvement of vision in the majority of patients with wet AMD when treated with ranibizumab.[3,4] After treatment, macular fluid and visual acuity often improve after only a few days.[3-5] On the basis of findings from phase 1 and 2 studies, dosing regimens for initial phase 3 studies were set at every 4 weeks, which subsequent research found to be appropriate on the basis of the half-life of the drug in the eye.[6] However, further studies, including the Phase IIIb, Multicenter, Randomized, Double-Masked, Sham Injection-Controlled Study of the Efficacy and Safety of Ranibizumab in Subjects with Subfoveal Choroidal Neovascularization with or without Classic CNV Secondary to Age-Related Macular Degeneration (PIER) and Prospective OCT Imaging of Patients with Neovascular AMD Treated with Intra-Ocular Lucentis (PrONTO), suggest that ranibizumab may be effective in many patients for significantly longer than 4 weeks after injection.[7,8]

Optical coherence tomography (OCT) is a noninvasive imaging technique that is useful in diagnosing and monitoring a number of different macular diseases before and after treatment, including patients with neovascular AMD treated with ranibizumab.[3-5,7,8] Qualitative assessment of OCT images show morphologic changes within the retina, whereas quantitative assessments, such as macular mapping, provide thickness measurements of the macula. In AMD, fluid has been described on OCT as diffuse retinal edema, intraretinal cysts, subretinal fluid, subretinal pigment epithelium (RPE) fluid, or serous pigment epithelial detachment.[3-5,7,8] Choroidal neovascularization (CNV) may be visualized on OCT as a highly reflective material above or below the RPE.[9]

Significant advances in OCT technology have allowed an increase of axial resolution. New light sources allow ultrahigh resolution OCT (UHR-OCT) and improved axial resolution from 10 to ~3 μm.[10] New methods of signal detection termed "spectral" or "Fourier domain"

imaging enabled an increase in imaging speeds by 50 to 100 times that of standard OCT systems. These improvements allow highly detailed assessment of intraretinal microanatomy and 3-dimensional (3D) image analysis.[11],[12]

Our group has combined these improvements in OCT to develop a high-speed UHR-OCT (hsUHR-OCT) prototype device for use in the ophthalmology clinic. The goal of this study was to use this prototype device to evaluate retinal microanatomy before and 1 month after intravitreal injection of ranibizumab for the treatment of neovascular AMD, when the drug has presumably had a substantial effect. Three-dimensional segmentation software was also used to calculate discreet subretinal volumes before and after treatment.

Materials and Methods

Classic OCT systems (OCT with time-domain detection) perform measurements of the echo time delay of backscattered or back-reflected light from tissue by using an interferometer with a mechanically scanned optical reference path. These instruments have been extensively studied in ophthalmology.[9],[13] New detection techniques known as spectral or Fourier domain detection measure the echo time delay of light by measuring the spectrum of the interference between light from the tissue and light from a stationary, unscanned, reference arm.[14-16] Because all of the light echoes from different axial positions in the tissue are measured simultaneously, rather than sequentially, detection sensitivity and imaging speed can be increased dramatically. This method has been well described in previous literature.[11,12,14-16]

The axial (longitudinal) image resolution of OCT is determined by a property of the light source known as the coherence length, which is inversely proportional to the bandwidth of the light source. To improve axial resolution, broad bandwidth light sources are required. We used a compact broadband superluminescent diode light source capable of approximately $3.5\,\mu$m axial resolution in the human eye. The incident light on the eye was 750 uW, the same exposure used in commercial ophthalmic OCT systems, consistent with the American National Standards Institute recommendations for safe exposure. Our prototype hsUHR-OCT system enables data acquisition rates of up to 25,000 axial scans per second, corresponding to acquisition of approximately 49 images (512 axial scans per image) per second. This hsUHR-OCT instrument has been described in detail.[11],[12] These studies were approved by the Massachusetts Institute of Technology Committee on the use of Humans as Experimental Subjects and the Institution Review Board of the Tufts Medical Center.

hsUHR-OCT imaging was performed on 12 eyes of 12 people with exudative AMD before and 1 month after intravitreal injection of ranibizumab. Snellen charts were used to record vision at all visits. Patients were diagnosed with thorough biomicroscopic fundus examination, fluorescein angiography (FA), and Stratus OCT (Carl Zeiss Meditec). Stratus OCT and hsUHR-OCT imaging were performed at all visits. The inclusion criteria were age more than 50 years and a diagnosis of exudative AMD. Exclusion criteria were the presence any macular pathology other than AMD and any prior treatments with an anti-VEGF agent in either eye.

Before injection, an eyelid speculum was placed and the injection site was cleaned with 5% povidone-iodine solution. Intravitreal injection of 0.5 mg ranibizumab was performed at 4 mm from the limbus in phakic eyes and 3.5 mm from the limbus in pseudophakic eyes. A drop of gatifloxacin or tobramycin ophthalmic solution was placed in the eye after injection, and intraocular pressure was measured 20 minutes after injection.

By using the prototype hsUHR-OCT, 3 types of scan protocols were performed in each eye. The first protocol acquires 3 high-definition 6-mm OCT images (8192 axial scans per image). The second protocol acquires 21 high-definition (2048 axial scans per image) images in a raster pattern covering a 6×6-mm area of the macula. The third protocol acquires 3D OCT data in a

dense raster pattern consisting of 180 images (512 axial scans per image) covering a 6×6-mm area. The corresponding volume element (voxel) size is 12×3×1.3 μm. Data sets from the second and third protocols may be used for applications such as volumetric rendering, OCT fundus image generation, and mapping.

Volumetric rendering of hsUHR-OCT data was performed using Amira version 3.1.1 software for personal computer (Mercury Computer Systems, Berlin, Germany). By using this software, features of interest within the OCT images were manually outlined and separated from the rest of the image data by a single operator (AJW). Built-in software algorithms also allow detection of signal thresholds within an image, permitting the tracing of similar image features with greater ease. Selected image features were traced and segmented throughout the entire image set, and the segmented data were compiled to form a 3D volume object of the region of interest. Delineation software was used to interpolate between images so that tracing did not need to be manually performed on each individual OCT image, and the interpolation was adjusted if needed. Three-dimensional volume objects could be displayed in addition to or separately from orthogonal OCT image slices from the same data set. To calculate the true volume represented by the object, the voxel size of the object of interest was expressed as a fraction of the total voxel size of the image set. For each hsUHR-OCT image set, we assumed dimensions of 6.0×6.0×1.3 mm for the total volume. The true volume of the object of interest could then be calculated.

In this study, we delineated 2 separate volumes using the Amira software. The first measurement included the volume of fluid and fibrovascular material between the outer boundary of the retina and Bruch's membrane. We refer to this measurement as the subretinal/RPE fluid volume. The second measurement was of the fibrovascular lesion. This was the moderately to highly reflective lesion that could be separated from the RPE and retina. Of note, in some cases the fibrovascular lesion volume was difficult to calculate because of the unclear delineation between the RPE and the lesion. Features included as part of the fibrovascular lesion were contiguous thickened reflective components compared with thinner, more normal areas of RPE. Often there was subretinal or sub-RPE fluid adjacent to the CNV lesion, which also helped to delineate the fibrovascular lesion. Fibrovascular lesions were for the most part below the RPE; however, some lesions extended more anteriorly into the RPE and subretinal space.

Microsoft Excel (Microsoft Corp, Redmond, WA) was used for data accumulation and analysis. Mean values and standard deviations were calculated for age, visual acuity, Stratus OCT thickness, and the 2 volumes calculated from hsUHR-OCT data. Visual acuities were converted to the logarithm of the minimum angle of resolution (logMAR) values for calculation of the mean. Foveal thickness on Stratus OCT was recorded as the central 1-mm circle of the macular map, generated by the regular macular thickness Stratus OCT mapping protocol. Two-tailed paired Student t tests were used for statistical analysis and generation of P values.

Results

Twelve eyes of 12 patients with exudative AMD were measured just before and 1 month after intravitreal injection with ranibizumab. There were 9 female and 3 male patients. The mean age was 80.7 years (range, 64 −97 years). One patient had been treated with photodynamic therapy 6 times before ranibizumab injection, and 1 patient previously received focal laser for juxtafoveal CNV. None of the eyes had received prior anti-VEGF treatment. Foveal thickness measurements acquired from the central circle on the Stratus OCT macular map ranged from 192 to 444 μm with a mean of 294 μm (±76 μm) before treatment with ranibizumab. Before treatment, visual acuity ranged from 20/40 to hand motions at 6 feet with a mean of 20/217 (logMAR 1.03±0.78).

All patients had some normalization of macular contour after ranibizumab injection, as well as a decrease in macular thickness on Stratus OCT. Foveal thickness on Stratus OCT ranged from 182 to 299 μm with a mean of 211 μm (± 20 μm) after treatment with ranibizumab. Visual acuity ranged from 20/20 to finger counting at 4 feet with a mean of 20/133 (logMAR 0.82 $\pm$ 0.60) after treatment. The decrease in foveal thickness on Stratus OCT was statistically significant ($P = .009$), and the increase in visual acuity approached statistical significance ($P = .126$).

On hsUHR-OCT, all eyes had a thickened and irregular RPE layer both before and after treatment. Bruch's membrane was visible in 9 of 12 eyes. Classic neovascular membrane components as visualized on FA appeared as highly reflective lesions anterior to the RPE on OCT. Occult membrane components were seen as moderately reflective areas between the RPE and Bruch's membrane. Focal interruptions in the inner/outer segment junction line overlying the CNV lesion were apparent in all 12 eyes before intravitreal ranibizumab and persisted 1 month after treatment. Nine of 12 eyes had focal areas of thinning of the outer nuclear layer overlying parts of the CNV lesion, all of which remained after treatment (see Figures 1 and 2 for examples of these findings).

A 3D rendering of the hsUHR-OCT data was possible both before and after treatment in 8 eyes from 8 patients (Fig 3). In 5 of these eyes, data from the 180-image protocol were used to calculate a volumetric rendering, whereas in the remaining 3 eyes, data from the 21-image protocol were used because of poor quality of the images from the 180-image protocol. Reasons for inability to render imaging data in 3D included poor signal (secondary to media opacities), poor patient cooperation, and out of range images resulting from patient movement, fixation movement, or a large amount of edema. Only 1 of these 8 eyes had received prior treatment for AMD; patient 6 had had focal laser.

Two volumes were calculated using the Amira software: the total volume between Bruch's membrane and the outer boundary of the retina (subretinal/RPE fluid volume), and the volume of the fibrovascular lesion. Volume results are listed in Table 1. The decrease in subretinal/RPE fluid volume was found to be statistically significant after treatment ($P = .011$). However, there was no statistically significant change in fibrovascular lesion volume after treatment ($P = .262$). An example of the limitation of CNV delineation is seen in patient 6 from Table 1. In this patient, the CNV volume measurement increased after treatment. This patient had a large volume of subretinal and sub-RPE fluid before treatment, which may have obscured the CNV lesion and caused underestimation with the initial measurement of CNV volume.

Discussion

Recent advances in OCT technology allow for increased image resolution and imaging speed. Increased axial resolution allows more accurate visualization of intra- and subretinal layers, particularly at the level of the photoreceptors and RPE. Increased imaging speeds enable acquisition of greater amounts of data, which can be used for precise fundus registration and 3D reconstruction of data. In this study, we used an hsUHR-OCT prototype to analyze intraretinal microanatomy in eyes with exudative AMD before and 1 month after injection with ranibizumab.

Food and Drug Administration approval of intravitreal injection of ranibizumab for all types of exudative AMD has led to a revolutionary shift in the paradigm for treatment of this disease. OCT data from the MARINA, Safety Assessment of Intravitreal Lucentis for AMD (SAILOR), PIER, and PrONTO studies show that stabilized or improved visual acuity in these patients was accompanied by a decrease in macular thickness and reduction of leakage of intraretinal

and subretinal fluid within days after injection. The size of the CNV lesion seemed to stabilize on FA in the treatment groups when compared with the control groups.[1-5,7,8]

Similar to the clinical trials listed previously, we found a significant reduction of retinal thickness on Stratus OCT 1 month after injection with ranibizumab. hsUHR-OCT demonstrated the intraretinal and subretinal fluid with increased clarity, as well as the choroidal neovascular lesions. Three-dimensional analysis of the subretinal/RPE space, which included subretinal and sub-RPE fluid, revealed a significant decrease in this volume 1 month after injection, whereas 3D analysis of fibrovascular lesion did not reveal a significant change in volume 1 month after injection. It seems, therefore, that the reduction in retinal thickness at 1 month after injection is primarily the result of reduction in permeability in the neovascular lesion, with a subsequent reduction in intraretinal and subretinal fluid, without reduction in the size of the lesion via anti-VEGF therapy.

VEGF is known to stimulate vascular permeability and angiogenesis; therefore, one should expect to see a reduction in intraretinal, subretinal, and sub-RPE fluid as a result of VEGF inhibition.[1,2] The lack of change in size of the fibrovascular lesion suggests that the lesion itself may be more resistant to regression, at least after 1 injection of ranibizumab. Undoubtedly, this fibrovascular lesion consists of multiple components, which may include aberrant blood vessels, fibrous tissue, serous fluid, and other exudative material. Certain components of the fibrovascular lesion may therefore be more resistant to anti-VEGF therapy, whereas other components may regress more slowly over time with repeat injections of ranibizumab.

hsUHR-OCT also demonstrated interesting findings of retinal microstructure in these patients. In most patients, Bruch's membrane became visible when the RPE was detached from it, either secondary to sub-RPE fluid or from the CNV lesion itself. In all patients, the RPE line was thickened and irregular. Similar findings of RPE irregularity and detachment from Bruch's membrane have been demonstrated in qualitative UHR-OCT analysis of eyes with nonexudative AMD and probably represents a combination of accumulation of drusenoid material and RPE clumping.[17] Classic components of CNV lesions appeared as hyperreflective lesions anterior to the RPE, and occult components were seen as moderately reflective lesions between the RPE and Bruch's membrane. This finding has been demonstrated on Stratus OCT and correlates with histopathologic studies.[18-20]

The hyperreflective line, anterior to the RPE line, representing the inner/outer segment junction of the photoreceptors (as described in previous UHR-OCT studies),[10,11] was discontinuous in areas overlying CNV in all 12 eyes. One month after treatment, the inner/outer segment junction remained discontinuous in all 12 eyes. In 9 of 12 eyes, the outer nuclear layer thinning was seen before treatment and persisted 1 month after injection. This finding suggests that, despite treatment, visual recovery 1 month after injection may be limited because of an initial insult to the photoreceptors by CNV.

Limitations of this study include small patient number, short follow-up, lack of automated volumetric delineation software, exclusion of 4 eyes from 3D volume rendering, and use of a commercially unavailable OCT prototype. The use of a larger number of patients may have shown a more significant change in fibrovascular lesion size after treatment not evident in this study. Longer follow-up time after multiple injections may show a reduction in fibrovascular lesion size that occurs later in the course of treatment and would help to determine if photoreceptor abnormalities persist over a longer period. Automated delineation of the fibrovascular lesion would eliminate operator error and allow more rapid volumetric calculation from visit to visit. However, it is still difficult to separate the fibrovascular lesion from the RPE or pockets of proteinaceous fluid in some cases. Six of 12 eyes could not be

included in 3D rendering because of media opacities, lack of cooperation, or out-of-range images, demonstrating the limitation of this technology when measuring eyes in patients with exudative AMD.

Although we used a hsUHR-OCT prototype in this study, new commercial spectral/Fourier domain OCT systems are now available from multiple manufacturers that provide 5 to 7-μm axial image resolutions and imaging speeds of 25 to 50,000 axial scans/second. Therefore, the methods and conclusions of this article (e.g., photoreceptor analysis and 3D reconstructions of OCT data) may likely be applied to future studies using commercially available spectral/Fourier domain OCT systems.

In future studies, photoreceptor anatomy may be more readily assessed and quantified, and could become an important prognostic factor for patients undergoing treatment for exudative AMD. Three-dimensional rendering of retinal and intraretinal structures may enable more detailed assessment of lesions, such as CNV. This may prove to be a useful method for tracking eyes over time as they respond to treatment. Longer-term studies using spectral/Fourier domain OCT imaging would help to understand how retinal and fibrovascular lesion anatomy changes after several ranibizumab injections.

hsUHR-OCT demonstrates a reduction of retinal thickness and normalization of retinal contour 1 month after intravitreal injection of ranibizumab for exudative AMD. This change is likely due to a decrease in permeability of the choroidal neovascular lesion, without a change in the size of the fibrovascular lesion itself. Photoreceptor disruption overlying areas of CNV is present in all eyes and may occur with the initial insult of the disease process, which likely does not resolve 1 month after treatment of these eyes with ranibizumab.

Acknowledgments

References

1. Andreoli CM, Miller JW. Anti-vascular endothelial growth factor therapy for ocular neovascular disease. Curr Opin Ophthalmol 2007;18:502–8. [PubMed: 18163003]

2. Brown DM, Regillo CD. Anti-VEGF agents in the treatment of neovascular age-related macular degeneration: applying clinical trial results to the treatment of everyday patients. Am J Ophthalmol 2007;144:627–37. [PubMed: 17893015]

3. Brown DM, Kaiser PK, Michels M, et al. ANCHOR Study Group. Ranibizumab versus verteporfin for neovascular age-related macular degeneration. N Engl J Med 2006;355:1432–44. [PubMed: 17021319]

4. Rosenfeld PJ, Brown DM, Heier JS, et al. MARINA Study Group. Ranibizumab for neovascular age-related macular degeneration. N Engl J Med 2006;355:1419–31. [PubMed: 17021318]

5. Kaiser PK, Blodi BA, Shapiro H, et al. MARINA Study Group. Angiographic and optical coherence tomographic results of the MARINA study of ranibizumab in neovascular age-related macular degeneration. Ophthalmology 2007;114:1868–75. [PubMed: 17628683]

6. Stewart MW. Predicted biologic activity of intravitreal bevacizumab. Retina 2007;27:1196–200. [PubMed: 18046224]

7. Fung AE, Lalwani GA, Rosenfeld PJ, et al. An optical coherence tomography-guided, variable dosing regimen with intravitreal ranibizumab (Lucentis) for neovascular age-related macular degeneration. Am J Ophthalmol 2007;143:566–83. [PubMed: 17386270]

8. Regillo CD, Brown DM, Abraham P, et al. PIER Study Group. Randomized, double-masked, sham-controlled trial of ranibizumab for neovascular age-related macular degeneration: PIER Study year 1. Am J Ophthalmol 2008;145:239–48. [PubMed: 18222192]

9. Hee MR, Baumal CR, Puliafito CA, et al. Optical coherence tomography of age-related macular degeneration and choroidal neovascularization. Ophthalmology 1996;103:1260–70. [PubMed: 8764797]

10. Drexler W, Morgner U, Ghanta RK, et al. Ultrahigh-resolution ophthalmic optical coherence tomography. Nat Med 2001;7:502–7. [PubMed: 11283681]

11. Srinivasan VJ, Wojtkowski M, Witkin AJ, et al. High-definition and 3-dimensional imaging of macular pathologies with high-speed ultrahigh-resolution optical coherence tomography. Ophthalmology 2006;113:2054–65. [PubMed: 17074565]

12. Wojtkowski M, Srinivasan V, Fujimoto JG, et al. Three-dimensional retinal imaging with high-speed ultrahigh-resolution optical coherence tomography. Ophthalmology 2005;112:1734–46. [PubMed: 16140383]

13. Huang D, Swanson EA, Lin CP, et al. Optical coherence tomography. Science 1991;254:1178–81. [PubMed: 1957169]

14. Leitgeb, R.; Hitzenberger, CK.; Fercher, A. Performance of Fourier domain vs. time domain optical coherence tomography.; Opt Express. 2003 [September 15, 2008]. p. 889-94.[serial online]Available at: http://www.opticsinfobase.org/abstract.cfm?URI=oe-11-8-889.

15. Yun, S.; Tearney, G.; Bouma, B., et al. High-speed spectral-domain optical coherence tomography at 1.3 μm wavelength.; Opt Express. 2003 [September 15, 2008]. p. 3598-604.[serial online]Available at: http://www.opticsinfobase.org/abstract.cfm?URI=oe-11-26-3598.

16. Choma, M.; Sarunic, M.; Yang, C.; Izatt, J. Sensitivity advantage of swept source and Fourier domain optical coherence tomography.; Opt Express. 2003 [September 15, 2008]. p. 2183-9.[serial online] Available at: http://www.opticsinfobase.org/abstract.cfm?URI=oe-11-18-2183.

17. Pieroni CG, Witkin AJ, Ko TH, et al. Ultrahigh resolution optical coherence tomography in non-exudative age related macular degeneration. Br J Ophthalmol 2006;90:191–7. [PubMed: 16424532]

18. Hughes EH, Khan J, Patel N, et al. In vivo demonstration of the anatomic differences between classic and occult choroidal neovascularization using optical coherence tomography. Am J Ophthalmol 2005;139:344–6. [PubMed: 15733999]

19. Coscas F, Coscas G, Souied E, et al. Optical coherence tomography identification of occult choroidal neovascularization in age-related macular degeneration. Am J Ophthalmol 2007;144:592–9. [PubMed: 17698019]

20. Lafaut BA, Bartz-Schmidt KU, Vanden Broecke C, et al. Clinicopathological correlation in exudative age related macular degeneration: histological differentiation between classic and occult choroidal neovascularisation. Br J Ophthalmol 2000;84:239–43. [PubMed: 10684831]
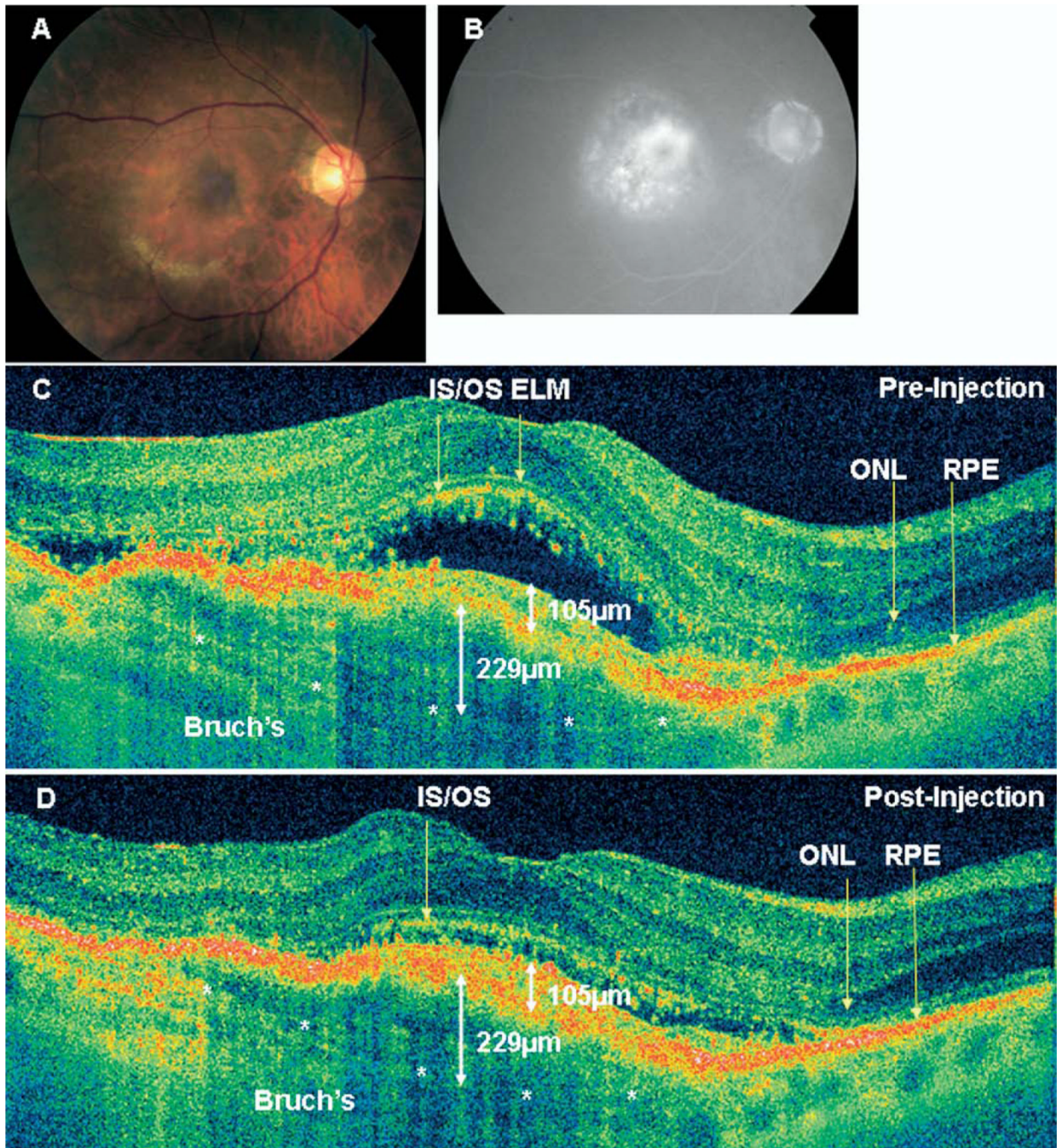
Figure 1.
A, Color fundus photograph from a 77-year-old woman with counting fingers vision at 4 feet (patient 3) before treatment. Hard exudates are seen in the inferior macula. **B,** Late-phase fluorescein angiogram demonstrates a primarily occult lesion with a classic component near the fovea. **C,** High pixel density (8192 axial scans) hsUHR-OCT image from the same eye before treatment. Note discontinuity of the inner/outer segment junction line and areas of outer nuclear layer thinning. Bruch's membrane is also demonstrated with the white asterisks. The occult component measures 229 μm in height, and the classic component measures 105 μm in height. **D,** High pixel density (8192 axial scans) hsUHR-OCT image from the same eye 1 month after treatment. Vision was counting fingers at 6 feet. Note persistent discontinuity of the inner/

outer segment junction line and thinning of the outer nuclear layer. Bruch's membrane is also demonstrated with the white asterisks. The occult and classic components of the neovascular membrane are demonstrated, and the same measurements are obtained as before treatment. The retinal contour has improved, primarily because of the resolution of subretinal fluid. ELM = external limiting membrane; hsUHR-OCT = high-speed ultrahigh resolution optical coherence tomography; IS/OS = inner/outer junction of photoreceptors; ONL = outer nuclear layer; RPE = retinal pigment epithelium.
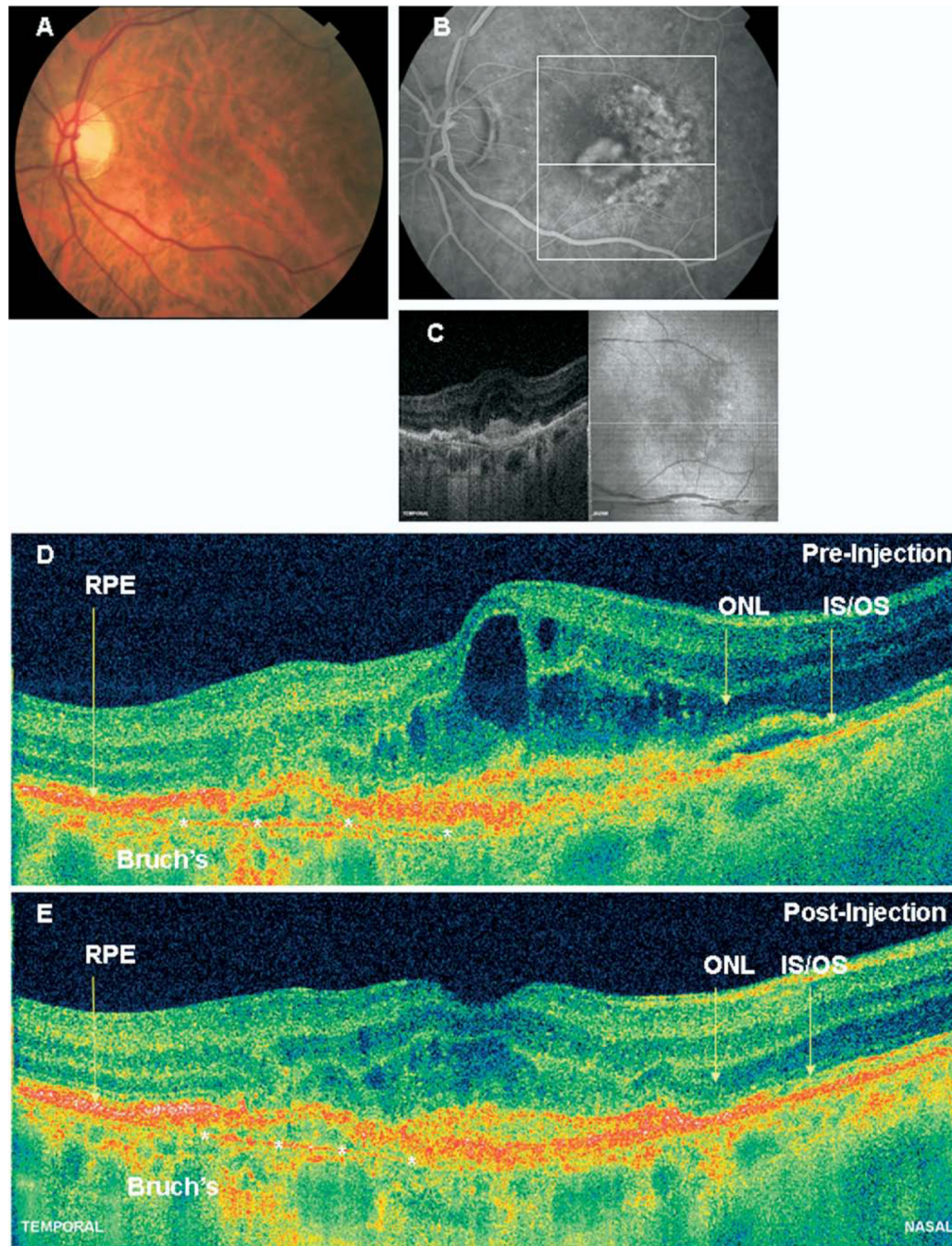
Figure 2.
A, Color fundus photograph from a 68-year-old woman with 20/400 vision (patient 8) before treatment. **B,** Midphase fluorescein angiogram demonstrates a primarily occult lesion with a classic component near the fovea. The white box demonstrates the OCT image area. **C,** Fundus reconstruction from hsUHR-OCT data, with precise registration of the OCT slice with the fundus image. **D,** High pixel density (8192 axial scans) hsUHR-OCT image of the same patient before treatment. Again, note discontinuity of the inner/outer segment junction line and areas of outer nuclear layer thinning. Bruch's membrane is also demonstrated with the white asterisks. Intraretinal fluid is evident. **E,** High pixel density (8192 axial scans) hsUHR-OCT image of the same patient 1 month after treatment with ranibizumab. Visual acuity remained at 20/400.

Again, note a persistent discontinuity of the inner/outer segment junction line and areas of thinning of the outer nuclear layer. Bruch's membrane is identified with the white asterisks. The retinal contour has improved, primarily from resolution of intraretinal fluid. 2D = 2-dimensional; hsUHR-OCT = high-speed ultrahigh resolution optical coherence tomography; IS/OS = inner/outer junction of photoreceptors; ONL = outer nuclear layer; RPE = retinal pigment epithelium.
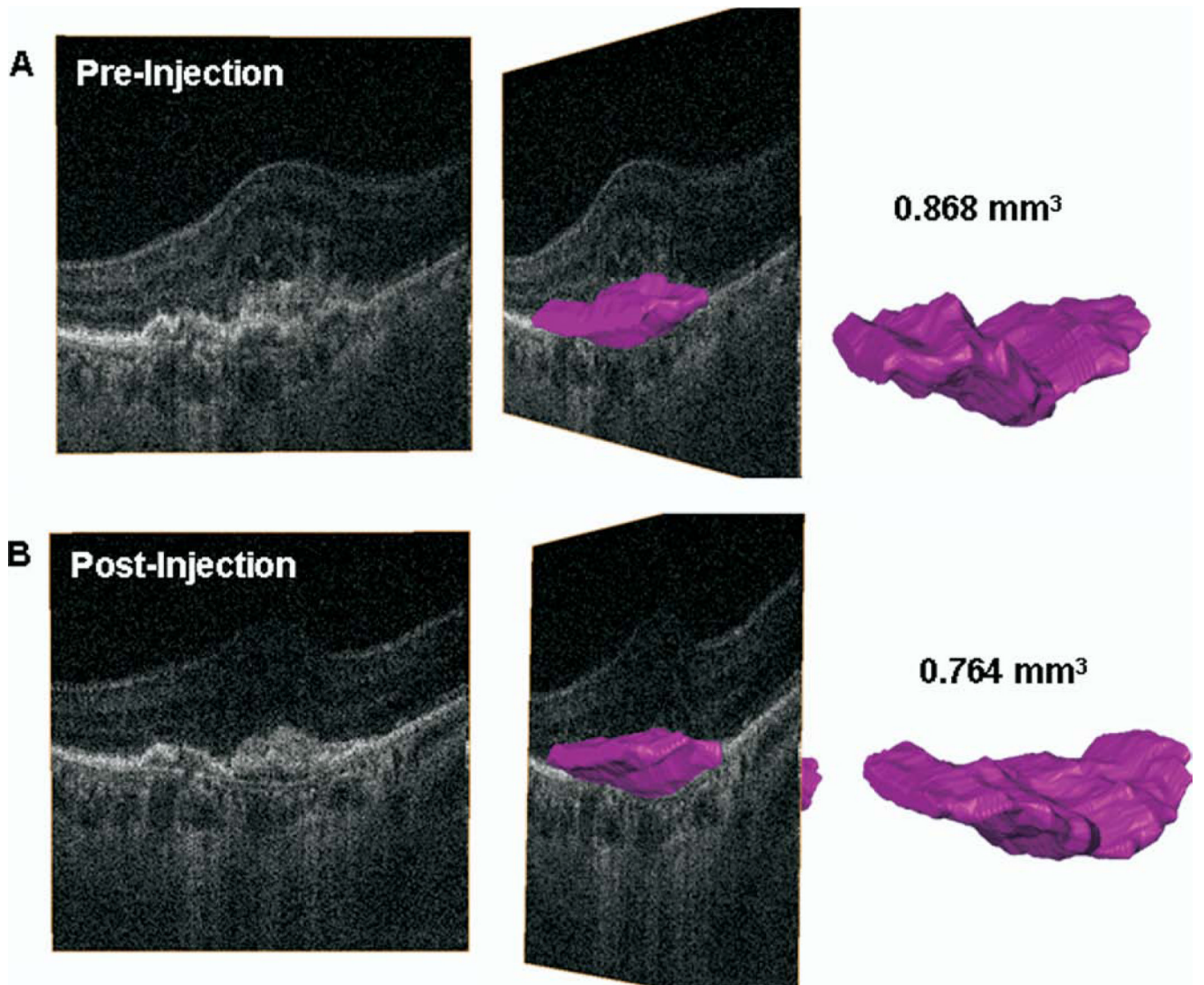
Figure 3.
A, Three-dimensional reconstruction of hsUHR-OCT data from before treatment. The pink object represents a volumetric reconstruction of the CNV lesion (both classic and occult components). Volume calculation shows the CNV to measure 0.868 mm^3. **B,** Three-dimensional reconstruction of hsUHR-OCT data from 1 month after treatment. The pink object represents a volumetric reconstruction of the CNV lesion (both classic and occult components). Volume calculation shows the CNV to measure 0.764 mm^3. CNV = choroidal neovascularization; hsUHR-OCT = high-speed ultrahigh resolution optical coherence tomography.

Table 1

Intraretinal Volumes[*]

	Subretinal/RPE Fluid Volume before Treatment	Subretinal/RPE Fluid Volume after Treatment	Fibrovascular Lesion Volume before Treatment	Fibrovascular Lesion Volume after Treatment
Patient 3	3.260	2.176	1.968	1.859
Patient 5	1.693	0.714	0.238	0.247
Patient 6	3.206	1.328	0.750	0.986
Patient 7	0.314	0.230	0.165	0.144
Patient 8	1.104	0.810	0.868	0.764
Patient 10	2.388	0.655	0.613	0.384
Patient 11	0.094	0.055	0.077	0.059
Patient 12	1.032	0.286	0.760	0.311
Mean	1.637	0.782	0.680	0.594
SD	1.221	0.690	0.601	0.599
P value	0.010		0.262	

RPE = retinal pigment epithelium; SD = standard deviation.

[*] Values are in mm^3.